Journal of Material Chemistry A

Supplementary Information

Fully sp^2-Carbon Connected Polymeric Frameworks with Rotatable Conformation-Enhanced Lithium-Storage Performance

Sidra Mushtaq,‡[a] Fancheng Meng,‡[a] Zixing Zhang,[a] Zhiheng Wang,[a] Biao Jiang,[a] Bai Xue,*[a] and Fan Zhang*[a]

[a] School of Chemistry and Chemical Engineering, State Key Laboratory of Metal Matrix Composites, Shanghai Jiao Tong University, 200240 Shanghai, P. R. China
*Corresponding authors; E-mail: fan-zhang@sjtu.edu.cn; bxue79@sjtu.edu.cn

Table of Contents

1. Experimental section

Experimental Procedures:

Synthetic procedures of 4-(tert-butyl)benzylidene-*s*-indacene-1,3,5,7(2H,6H)-tetraone (model compound)

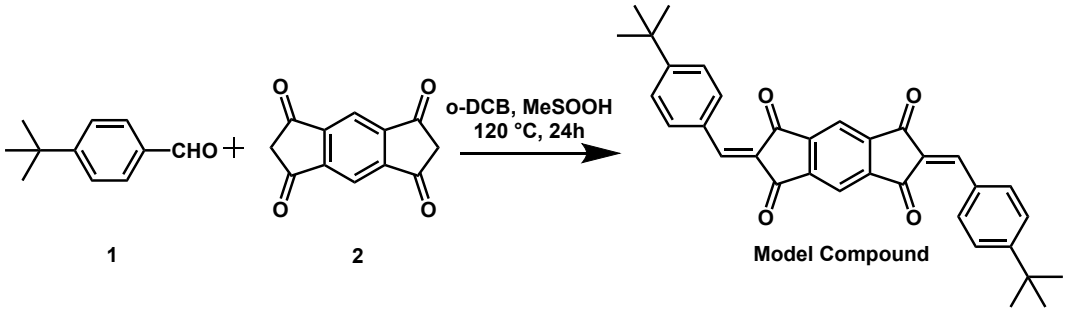

Scheme S1. Synthetic route for the model compound

s-indacene-1,3,5,7(2H,6H)-Tetraone (2), (1 mmol), 4-tert-butylbenzaldehyde (1) , 2 mmol) were employed in a flask with o-DCB (15ml) and stirred under a nitrogen atmosphere. The catalyst (1-2ml) was then added dropwise, the mixture was Freez-Pump-Thawed at least three times and the mixture was heated at 120 °C for 24 hours. After cooling down the reaction mixture to room temperature, the o-DCB was removed, and the crude product was extracted. After removal of the solvent, the solid residue was collected, and further purified by column chromatography in P.E/EtOAc (4:1) to afford the pure model compound as a yellow powder. Yield: 92%. ^{1}H NMR (400 MHz, $CDCL_3$) δ 8.58 (t, 1H), 8.50 (d, 2H), 8.04 (s, 1H), 7.61 (d, 2H), 1.41 (s, 9H).

Synthetic procedures for intermediates, key Dimer, and Material Synthesis:

Synthesis of Monomer TP-Ald:

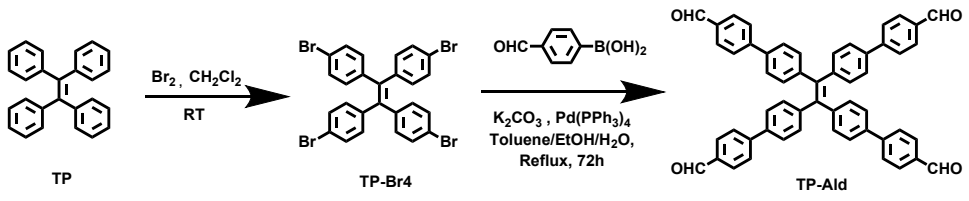

Scheme S2. Synthetic route for the monomer TP-Ald

1) Synthesis of TP-Br4:

Tetraphenylethylene (TPE) (1.62 g, 4.90 mmol) was dissolved in 50 ml of CH_2Cl_2 in a round flask, followed by the dropwise addition of 2 ml of Br_2 in 10 ml of CH_2Cl_2. The

mixture was stirred at 50 ˚C overnight and then quenched with a saturated aqueous solution of hydroxylamine hydrochloride. The aqueous solution was then extracted with CH_2Cl_2. The organic layer was dried over $MgSO_4$, filtered, and evaporated. The solid was washed with ethanol to yield white powder (Yield: 94%).

2) Synthesis of TP-Ald:

Tetrakis(4-bromophenyl)ethylene TP-Br4 (1 mmol), 4-formylphenyl boronic acid (6 mmol), and K_2CO_3 (12 mmol) were dissolved in Toluene/ethanol/water (50/20/10 ml) in schlenk flask, and nitrogen bubbling was provided for one hour. After N_2 bubbling, $Pd(pph_3)_4$ (15 mg) was added and then heated at 90 ˚C for three days. After completion of the reaction, solvents were removed by evaporation, and the yellowish-green solid was collected by the addition of MeOH/P.E and recrystallization from $CHCl_3$ (Yield: 84%).

Synthesis of Monomer BF-Ald:

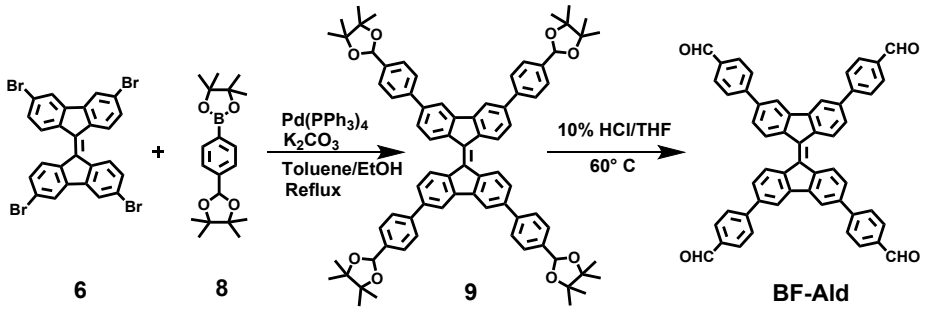

Scheme S3. Synthetic route for the monomer BF-Ald

The key intermediate (9,9-BF-4Br) (6) was synthesized in our previous research work in our group, according to the literature.[1-4]

1) Synthesis of (4,4,5,5-tetramethyl-2-[4-(4,4,5,5-tetramethyl-1,3-dioxolan-2-yl)phenyl]-1,3,2-dioxaborolane) 8:

A solution of 4-formylphenylboronic acid (7) (610 mg, 6.67 mmol), 2,3-dimethyl-butane-2,3-diol (3.94 g, 33.34 mmol), and a catalytic amount of *p*-toluenesulfonic acid in toluene (40 ml) was heated at reflux by using a Dean-Stark receiver for 3 hour. The reaction mixture was then washed with water (3*100 ml), dried, and concentrated. The product was purified over silica gel (petroleum ether/ethyl acetate, 9:1) to give the desired product as colorless needle-shaped crystals (Yield: 70%).

2) Synthesis of 3,3',6,6'-tetrakis(4-(4,4,5,5-tetramethyl-1,3-dioxolan-2-yl)phenyl)-9,9'-bifluorenylidene 9:

$Pd(dppf)Cl_2 \cdot CH_2Cl_2$ (111 mg, 0.137 mmol), **6** (682 mg, 2.05 mmol), and K_2CO_3 (946 mg, 6.85 mmol) were added to a solution of **8** (620 mg, 1.37 mmol) in toluene/MeOH (1:1, 10 ml) in a microwave vial. The resulting mixture was heated at 90 °C for 3 days. After cooling to room temperature, the reaction mixture was poured into water and extracted with ethyl acetate. The organic phase was washed with water (3*150 ml), dried, filtered, and concentrated under reduced pressure. Flash chromatography purification (cyclohexane/ethyl acetate, 4:1) gave the product as shiny reddish solid (Yield: 82%).

3) Synthesis of 4,4',4'', 4'''-([9, 9'-bifluorenylidene]-3, 3', 6, 6'-tetrayl) tetrabenzaldehyde (BF-Ald):

Compound **9** (300 mg) was dissolved in 10 % HCl/THF (1:2, 30 ml)). The mixture was heated at 60 °C for 12 hours and then poured into the water after the completion of the reaction. Ethyl acetate was added, and the organic layer was washed with water until neutral pH, dried with anhydrous Na_2SO_4, and filtered. The solvent was removed under reduced pressure, and purification by column chromatography, followed by crystallization from Methanol/DCM gave the pure product as purplish solid (Yield: 81%).

Synthesis of *s*-Indacene-1,3,5,7(2H,6H)-tetraone (3):

The linker 3 was synthesized according to the literature and the characterization data well matched with the literature.[5]

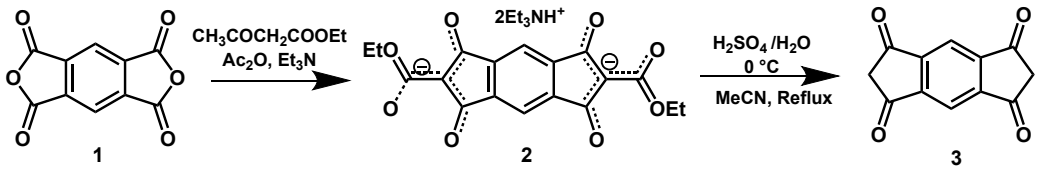

Scheme S4. Synthetic route for the *s*-Indacene-1,3,5,7(2H, 6H)-tetraone

2. Screening results of polymers

Table S1. Screening of reaction conditions with different catalysts and temperatures for the synthesis of TPT-CMP.

Sample	Solvent	Temperature (°C)	Catalyst	S.A $_{BET}$ (m^2 g^{-1})
1	Chloroform	120	Piperidine	52.12
2	DMF	150	Piperidine	--
3	o-Dcb	150	Piperidine	39.81
4	o-Dcb/n-BuOH (1:1)	150	Acetic acid	25.04
5	DMF	150	Acetic acid	--
6	n-BuOH	120	AcOH /water	44.80
7	o-Dcb/n-BuOH (2:1)	120	AcOH /water	46.21
8	o-Dcb/n-BuOH (1:2)	120	AcOH /water	81.33
9	o-Dcb	180	MSA	535.92
10	o-Dcb/n-BuOH (1:2)	180	MSA	29.70
11	o-Dcb/n-BuOH (2:1)	180	MSA	485.44
12	DMF/o-Dcb (1:2)	180	MSA	21.91

*All reactions were conducted for 72 h under nitrogen protection, (DMF= dimethylformamide, o-DCB= o-dichlorobenzene, n-BuOH= n-butanol, MSA= methanesulphonic acid, AcOH= acetic acid)

3. Elemental analysis of synthesized polymers

Table S2. Elemental analysis of TPT-CMP and BFT-CMP.

Elements	TPT-CMP (Expt./Calc.)	BFT-CMP (Expt./Calc.)
C (wt. %)	80.01/77.13	80.30/73.85
O (wt. %)	16.02/14.34	16.14/19.01
H (wt. %)	3.80/4.35	3.56/4.35

4. X-ray photoelectron spectroscopy

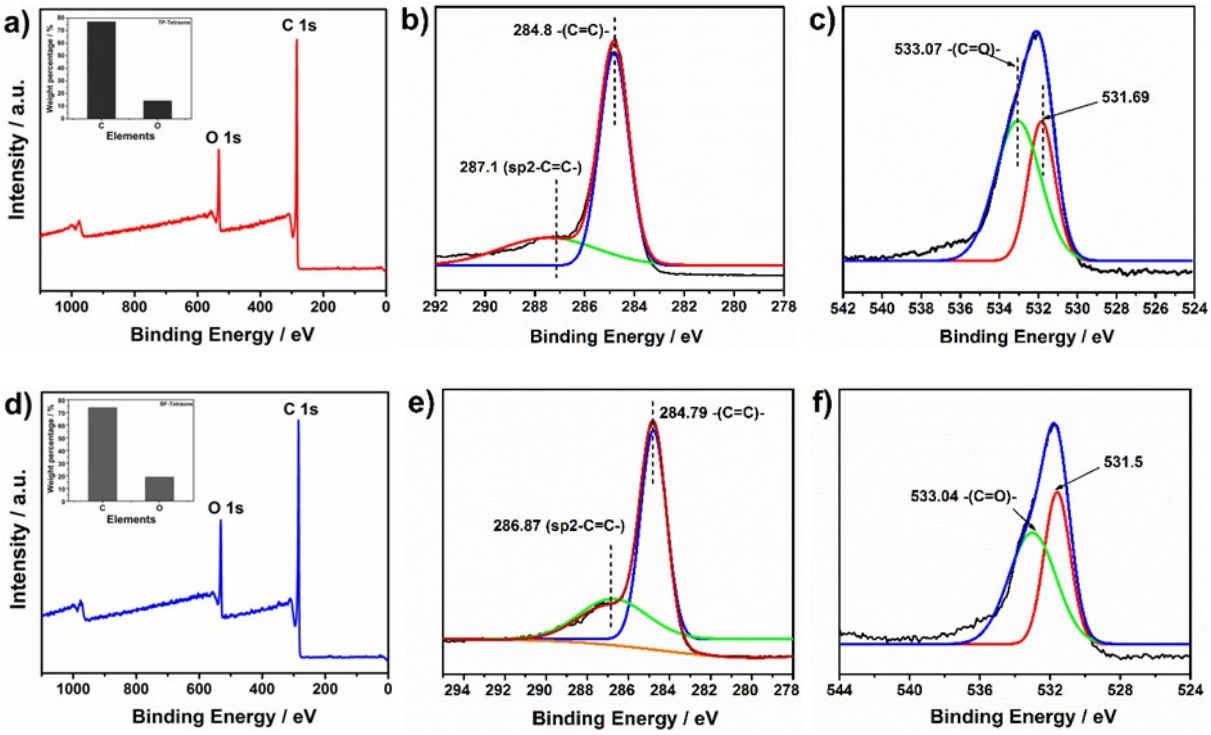

Fig. S1 XPS spectra of the polymers: a, d) Survey scans of TPT-CMP and BFT-CMP, b,c,e,f) high-resolution scans of C 1s and O 1s and the mass contents (insets).

5. DRS UV-Vis absorption spectra of polymers and monomers

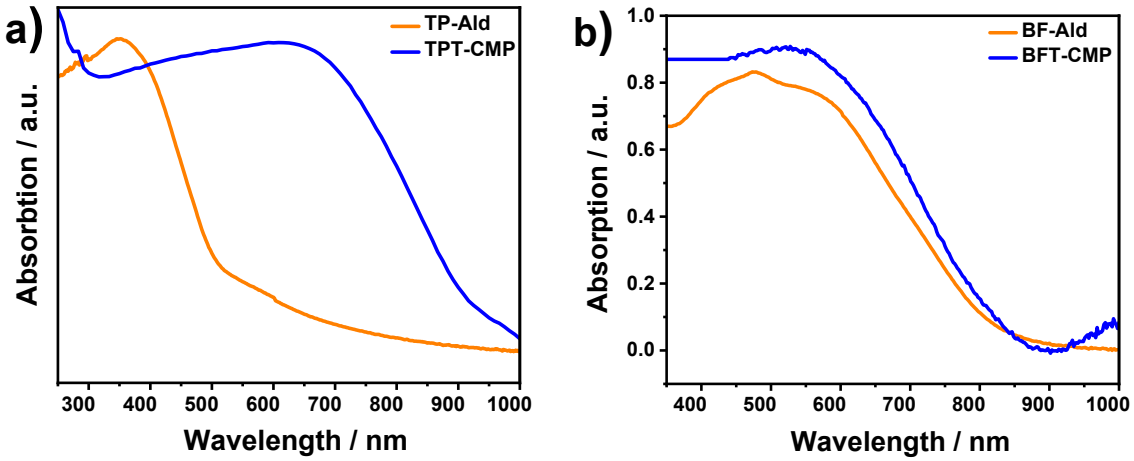

Fig. S2 UV/vis DRS spectra of TPT-CMP, BFT-CMP, and their respective monomers.

6. XRD analysis of as-synthesized polymers

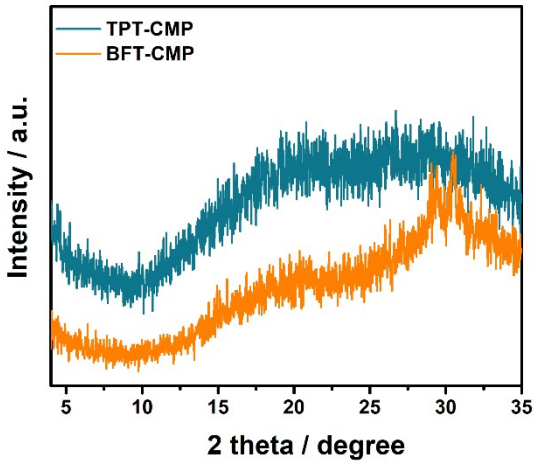

Fig. S3 Experimentally observed PXRD patterns of TPT-CMP and BFT-CMP polymers.

7. Nitrogen physisorption analysis and Pore size distribution profiles of polymers

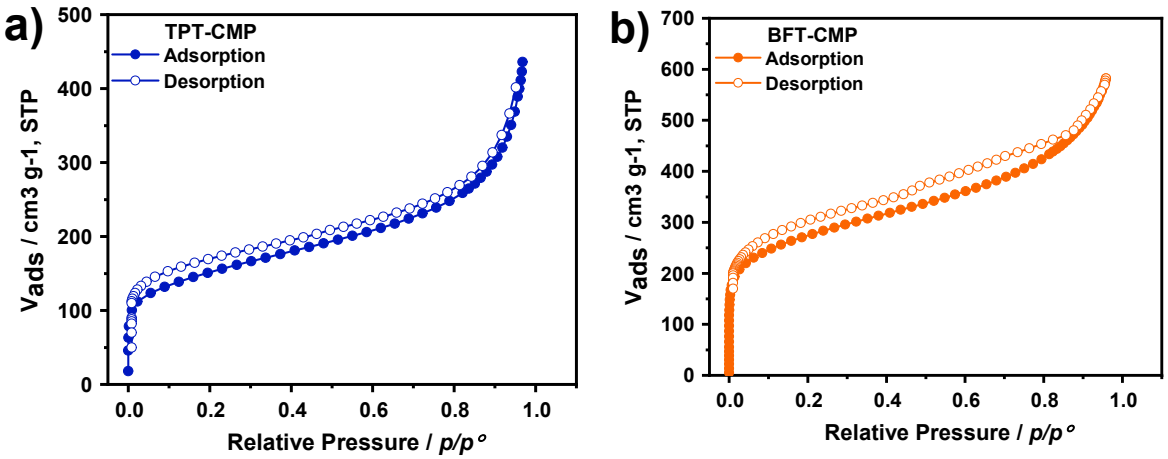

Fig. S4 Nitrogen sorption isotherms for as-synthesized polymers TPT-CMP and BFT-CMP.

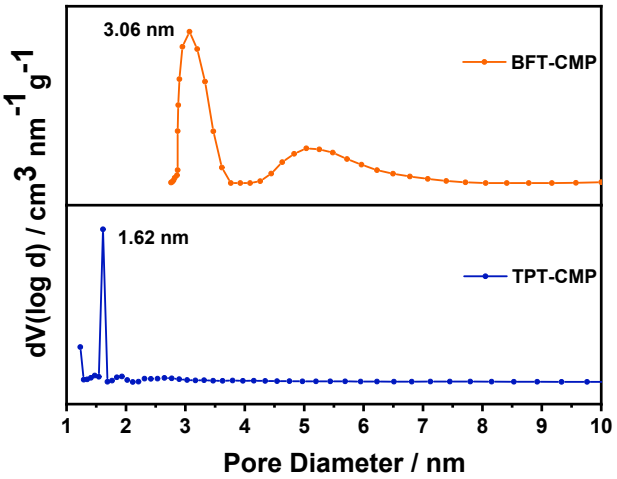

Fig. S5 Pore size distribution profiles of TPT-CMP and BFT-CMP polymers.

8. Scanning electron microscopy (SEM) images and Transmission electron microscopic (TEM) images

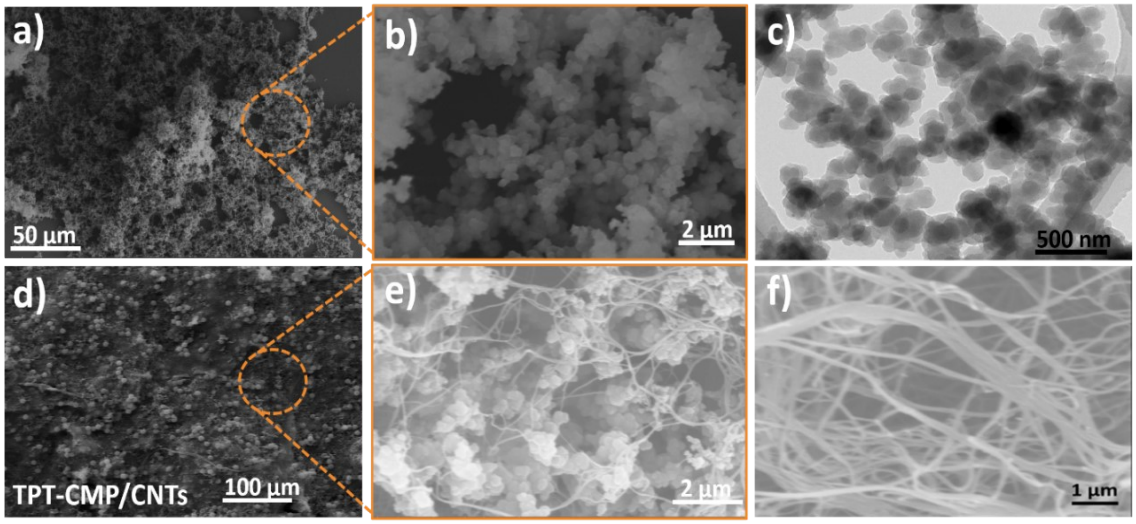

Fig. S6 Morphologies of TPT-CMP polymer and TPT-CMP/CNTs composite, a) SEM image of TPT-CMP and its b) magnified image, c) TEM image of TPT-CMP, d) SEM image of TPT-CMP/CNTs composite and its magnified image, e) showing CNTs wrapped TPT-CMP composite morphology with a uniform arrangement of an immobilized network, f) SEM morphology of CNTs.

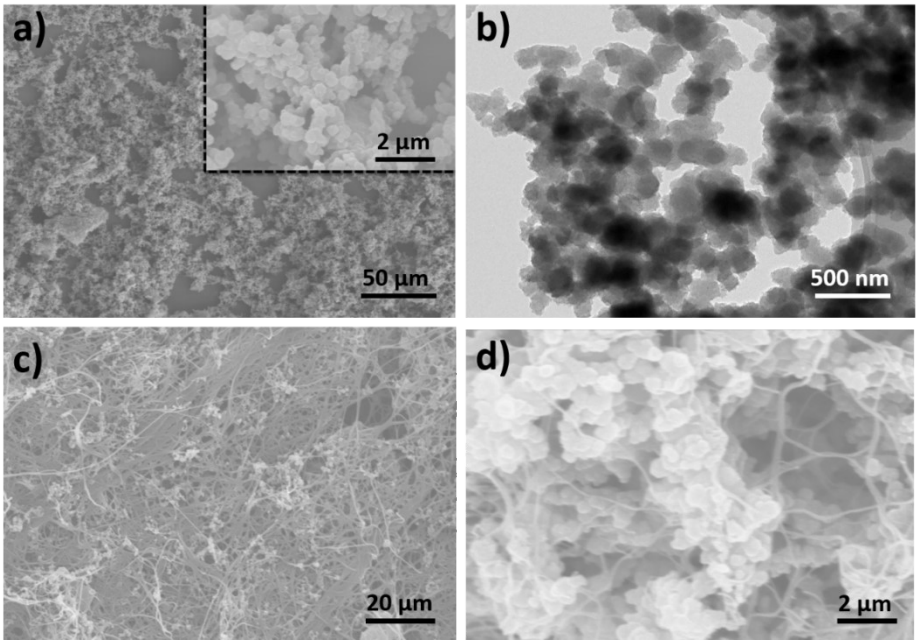

Fig. S7 SEM morphologies of BFT-CMP and its composites BFT-CMP/CNTs, a) SEM image of BFT-CMP polymer (inset magnified image), b) TEM image of BFT-CMP polymer, c) SEM image of BFT-CMP/CNTs composite showing the distribution of active material and CNTs network, d) CNTs wrapped BFT-CMP composite morphology.

9. Electrochemical tests

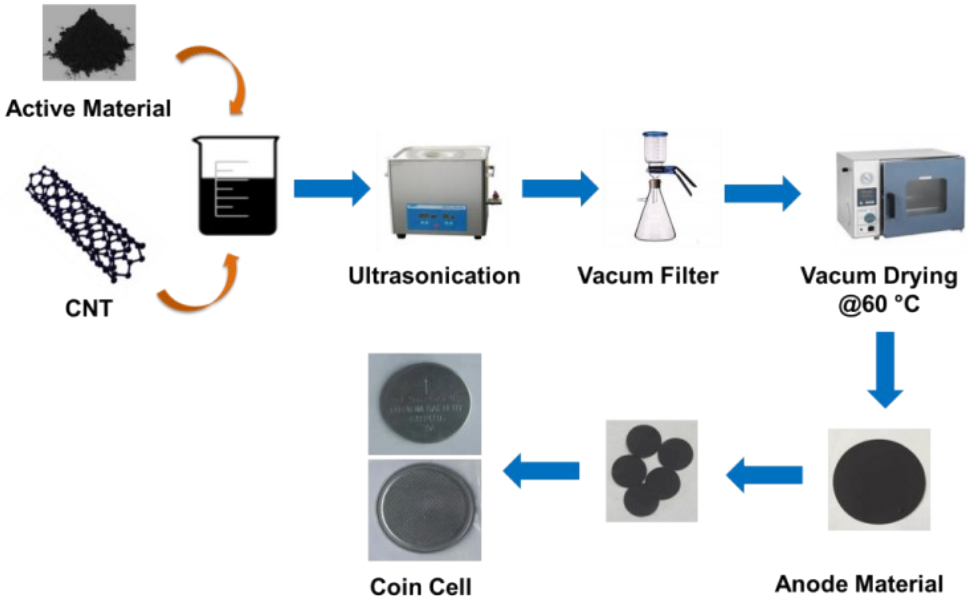

Fig. S8 The schematic illustration of the fabrication process for the coin cell type Li-ion battery.

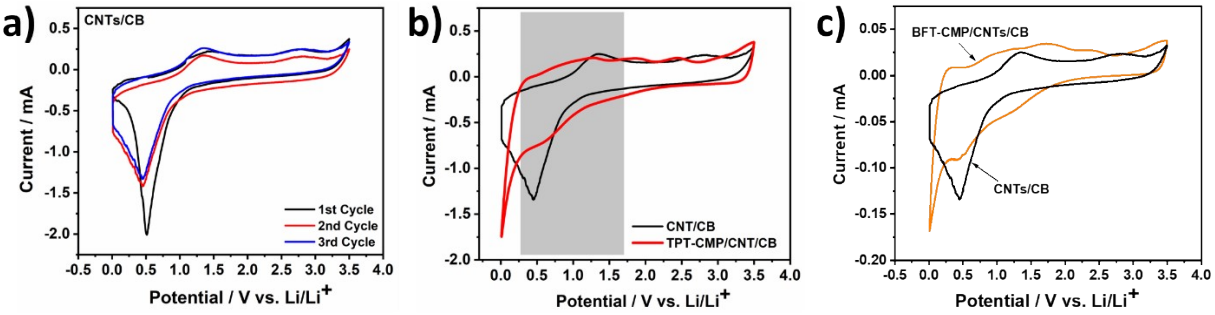

Fig. S9 a) CV profiles of CNTs/CB, Comparative CV curves of b) CNT/CB and TPT-CMP/CNT/CB and c) CNT/CB and BFT-CMP/CNT/CB.

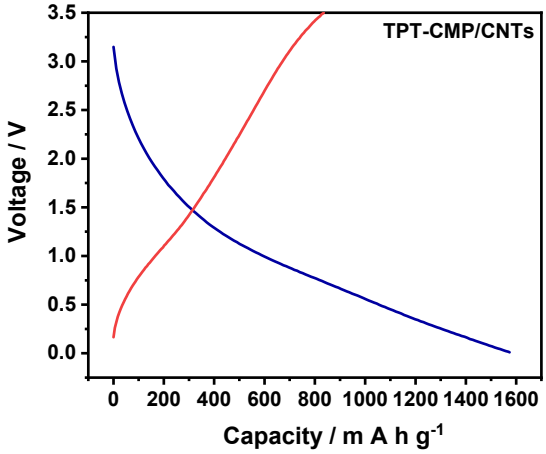

Fig. S10 Charge/discharge curves of TPT-CMP/CNT electrodes at a rate of 25 m A g^{-1}.

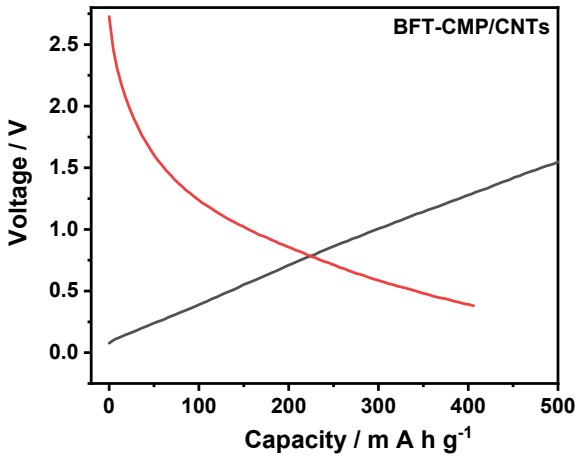

Fig. S11 Charge/discharge curves of BFT-CMP/CNT electrodes at a rate of 25 m A g^{-1}.

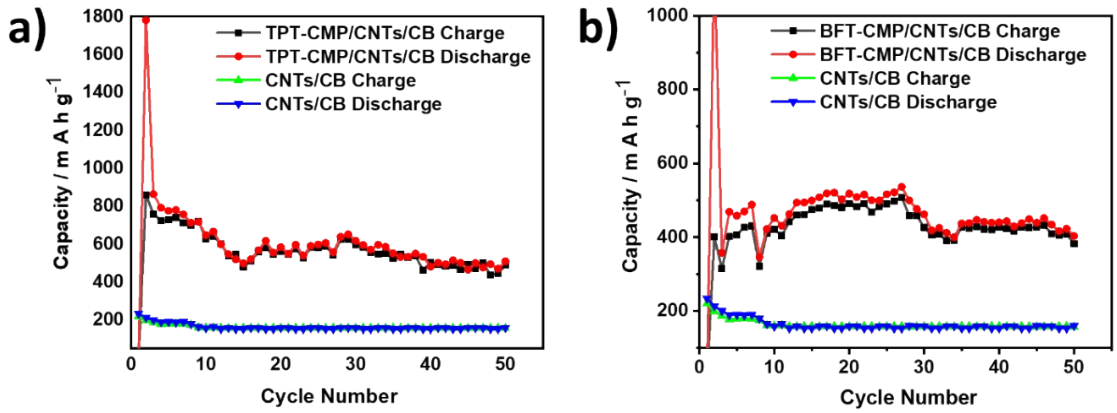

Fig. S12 Capacity retention of a) TPT-CMP/CNT/CB electrodes and CNT/CB electrodes, b) BFT-CMP/CNT/CB electrodes and CNT/CB electrodes.

Calculation of CNT/CB capacity contribution in the composite electrodes

The capacity contribution of CNT/CB in (TPT-CMP/CNT/CB and BFT-CMP/CNT/CB) composites were calculated by following equation (Eq: S1);

$$Composite\ specific\ capacity = (polymer\ specific\ capacity \times polymer\ mass + CNT/CB\ specific\ capacity \times CNT/CB\ mass)/(Polymer\ mass + CNT/CB\ mass) \quad \text{Eq: S1}$$

$$\text{Capacity contribution of CNTs/CB} = (CNT/CB\ capacity \times CNT/CB\ mass)/(Polymer\ mass + CNT/CB\ mass)$$

$$= (246\ mAh.g^{-1} \times\ 30\ \%)/(70\ \%\ +\ 30\ \%)$$

$$= 73.8\ \text{mAh g}^{-1}$$

Capacity contribution of CNT/CB in (TPT-CMP/CNT/CB and BFT-CMP/CNT/CB) composite electrodes is 73.8 mAh g^{-1}, at current density of 100 mA g^{-1}.

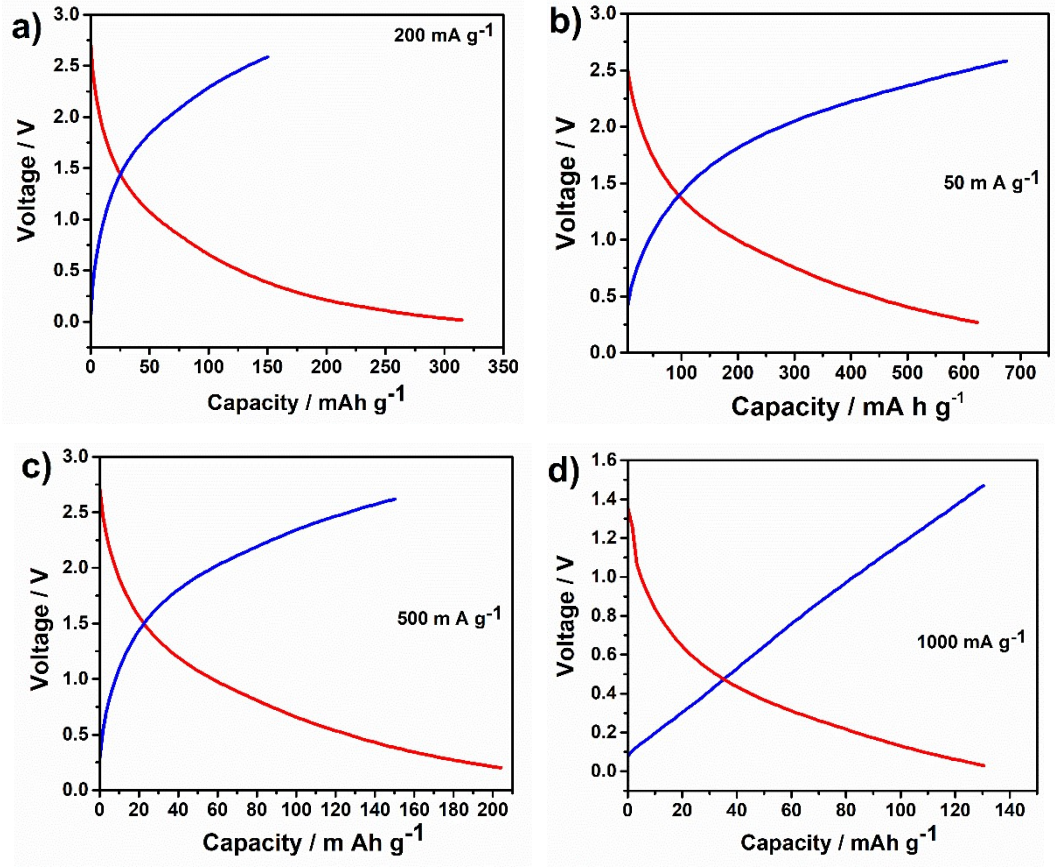

Fig. S13 Charge/discharge curves of TPT-CMP/CNT electrodes at different rates

Table S3. Performance of reported carbonyl-based electrode materials for lithium-ion batteries.

Polymer composite	Mass ratio of active materials in electrode	Specific capacity mAh g^{-1}	Cyclic stability	Reference
Poly dihydroxy anthraquinone)	50%	101 at 40 mA g^{-1}	129 mAh g^{-1} after 50 cycles at 40 mA g^{-1}	[6]
PI/CNT nanocomposite	85%	25 at 0.1C. (1C=273 mA g^{-1})	90 mAh g^{-1} after 300 cycles	[7]
PI/CNT films	100%	226 at 0.1C. (1C=443 mA g^{-1})	175 mAh g^{-1} after 200 cycles at 0.5C	[8]
3,4,9,10-perylenetetracarboxylicacid dianhydride	80%	131 at 100 mA g^{-1}	123 mAh g^{-1} after 200 cycles at 100 mA g^{-1}	[9]
Dimethoxy-1,4-benzoquinone	40%	312 at 10 mA g^{-1}	250 mAh g^{-1} after 10 cycles at 10 mA g^{-1}	[10]
PI	60%	200 at 0.1C. (1C=405.8 mA g^{-1})	170 mAh g^{-1} after 100 cycles	[11]
Poly (anthraquinonyl sulfide)	40%	218 at 0.1C. (1C=492 mA g^{-1})	198 mAh g^{-1} after 200 cycles at 0.1C	[12]
3D graphene Network supported PI	80%	175 at 0.1C. (1C=443 mA g^{-1})	101 mAh g^{-1} after 150 cycles at 0.5C	[13]
PI/MG	90%	625.7 at 100 mA g^{-1}	612.3 mAh g^{-1} after 100 cycles	[14]
TPT-CMP/CNT/CB	70%	1781 mAh g^{-1} at 25 mA g^{-1}	550.1 mAh g^{-1} after 50 cycles	**This Work**
BFT-CMP/CNT/CB	70%	1163 mAh g^{-1} at 25 mA g^{-1}	407 mAh g^{-1} after 50 cycles	

10. NMR spectra and Maldi-Tof MS spectra of intermediates and key monomers

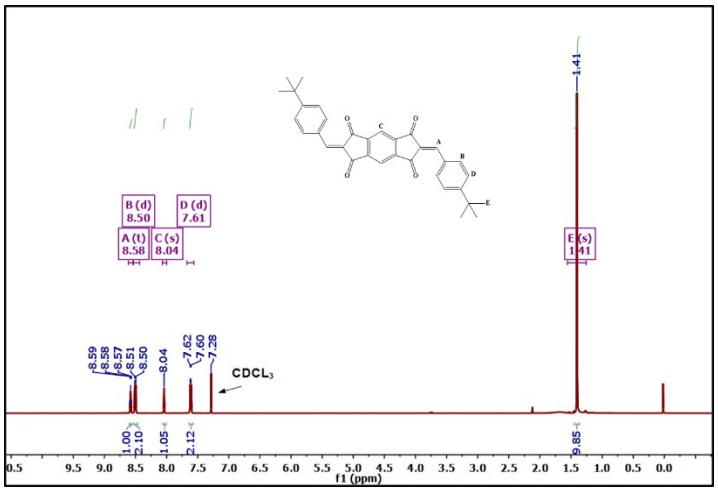

Fig. S14 ^{1}H-NMR spectra of the model compound.

NMR spectra and Maldi-Tof MS spectra of Monomer 1 and intermediates:

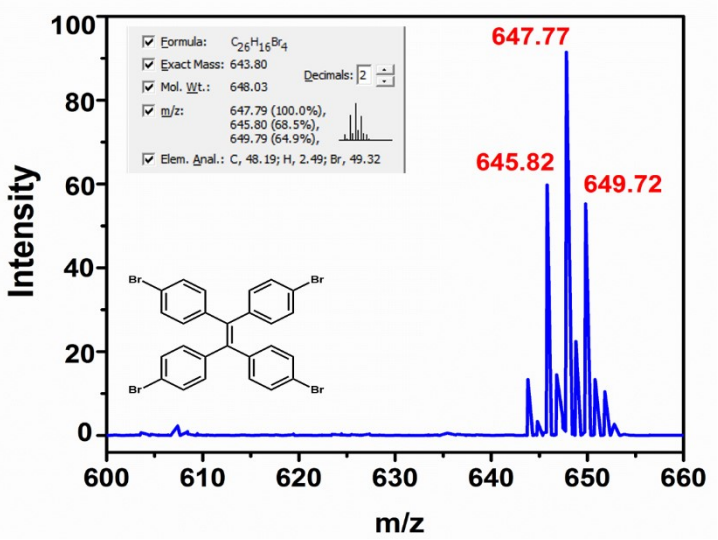

Fig. S15 Maldi-Tof MS spectra of TP-Br4.

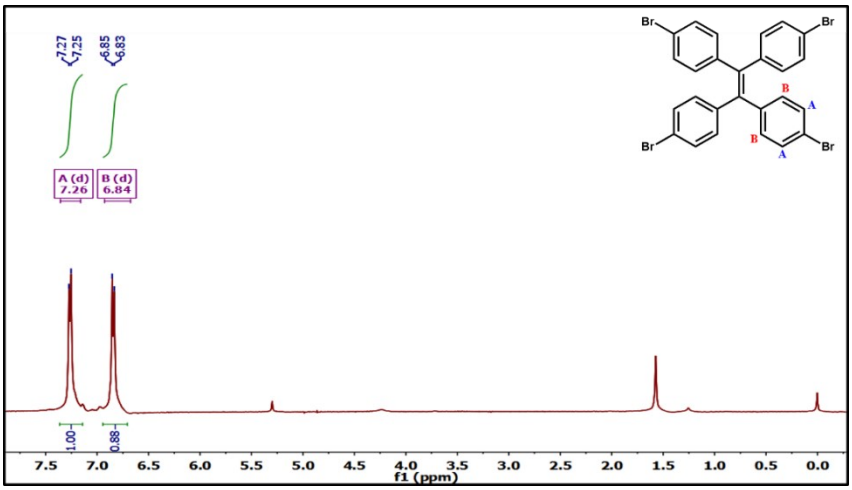

Fig. S16 [1]H-NMR spectra of TP-Br4.

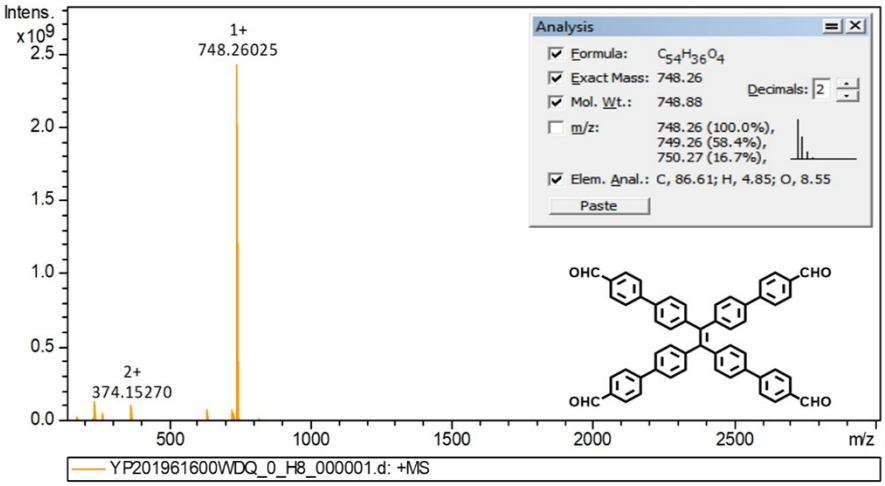

Fig. S17 Maldi-Tof MS spectra of TP-Ald.

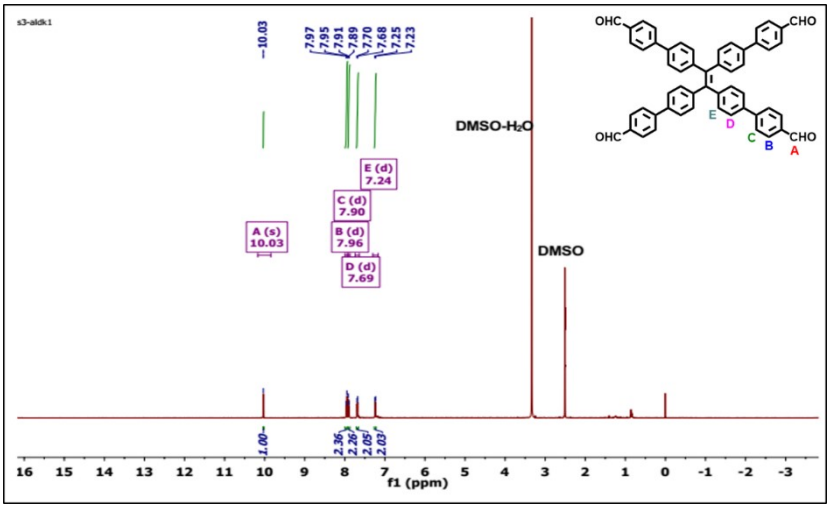

Fig. S18 [1]H-NMR spectra of TP-Ald.

NMR spectra and Maldi-Tof spectra of Monomer 2 and intermediates:

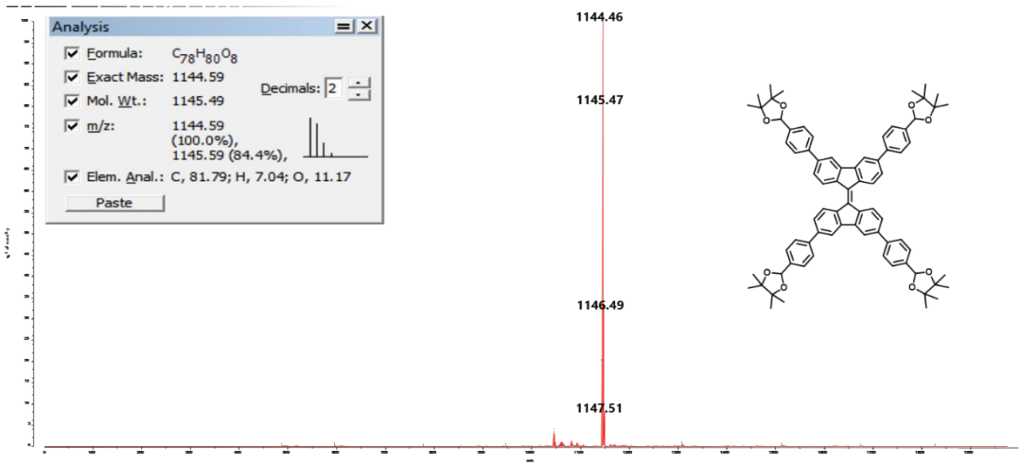

Fig. S19 Maldi-Tof MS spectra of 9.

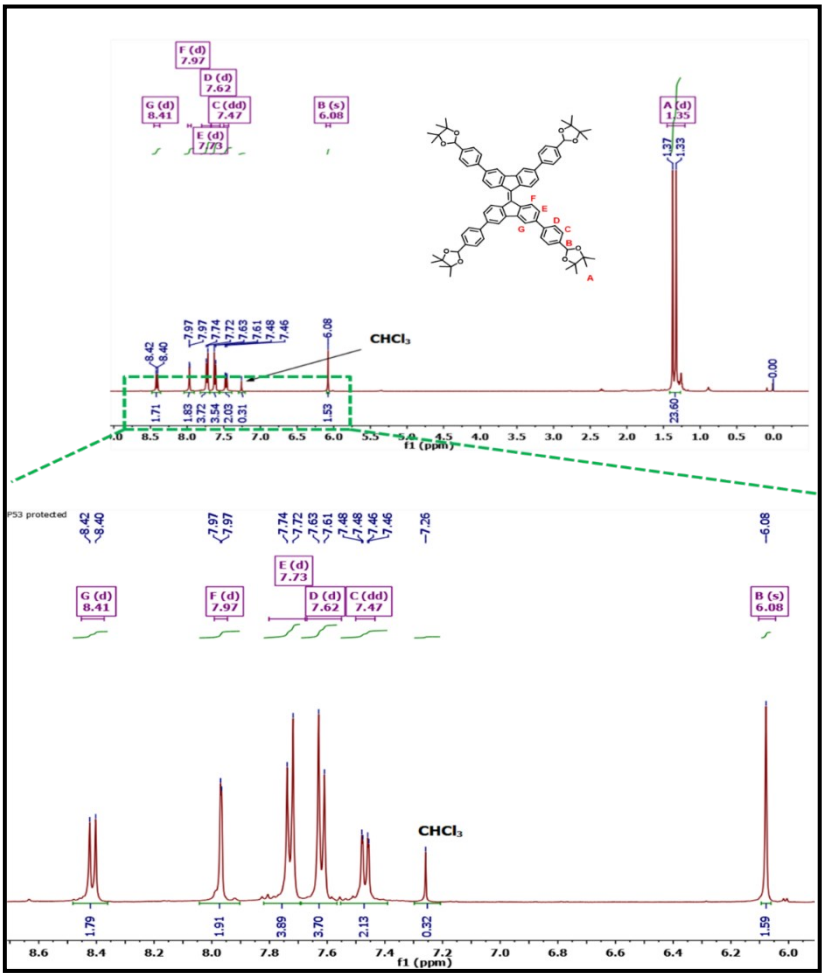

Fig. S20 ^{1}H-NMR spectra of 9.

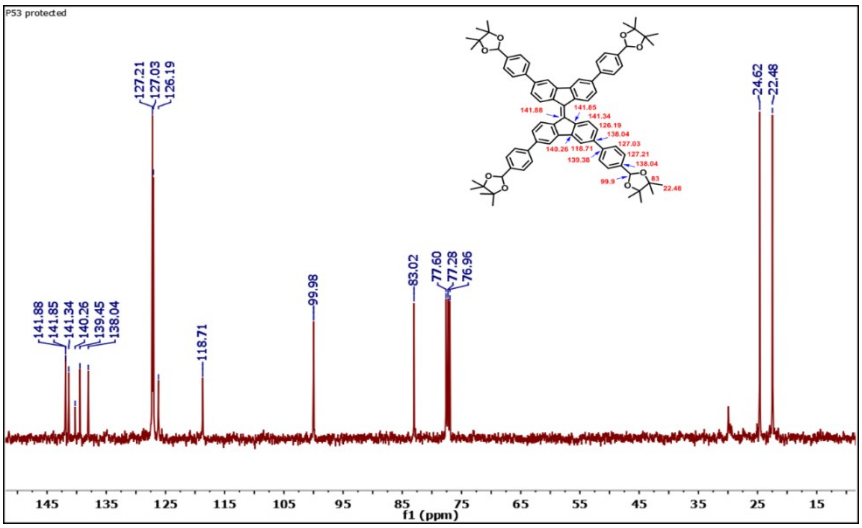

Fig. S21 ^{13}C-NMR spectra of 9.

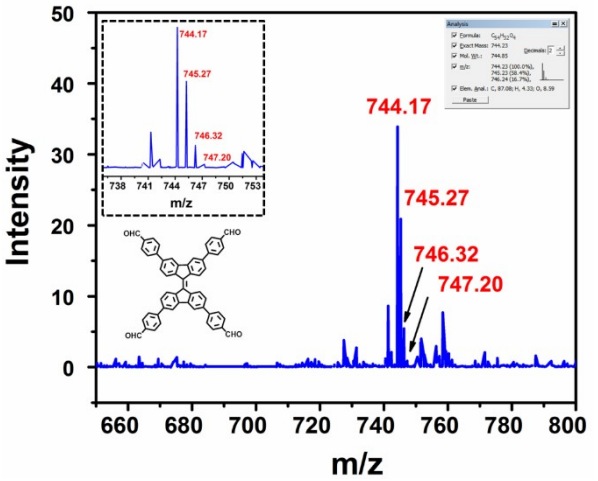

Fig. S22 Maldi-Tof MS spectra of BF-Ald.

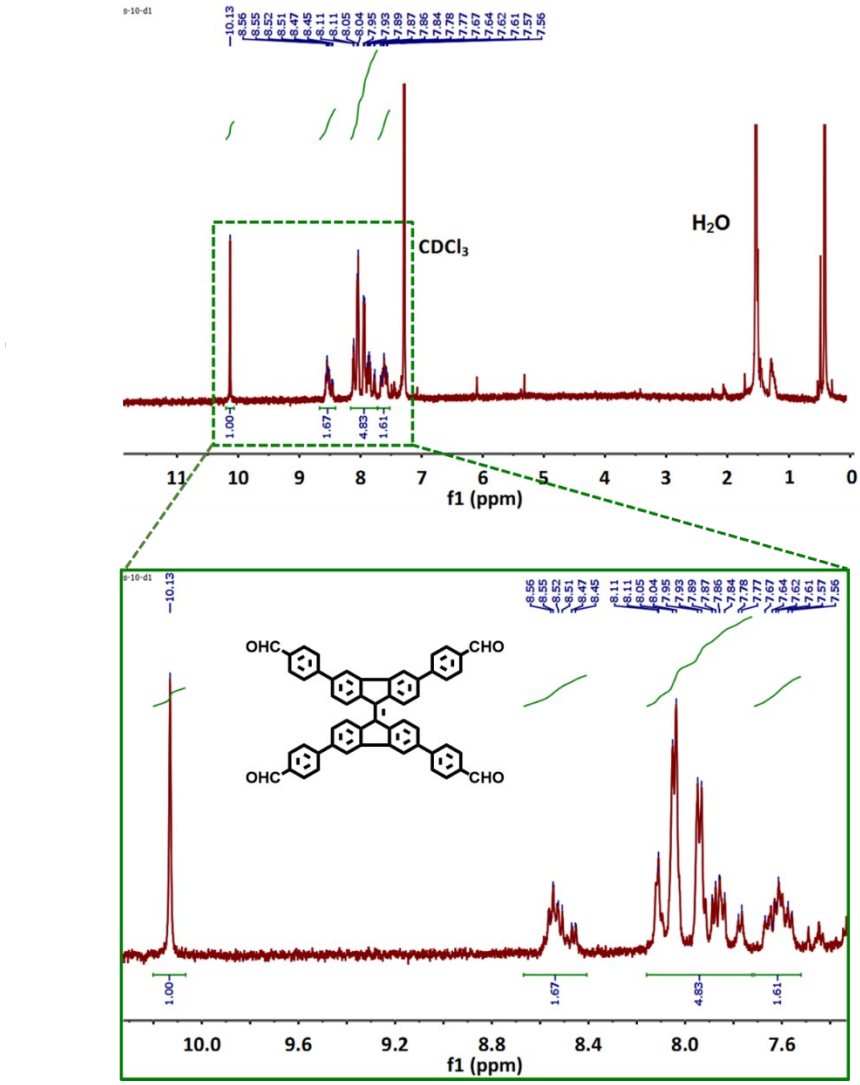

Fig. S23 ^{1}H-NMR spectra of BF-Ald.

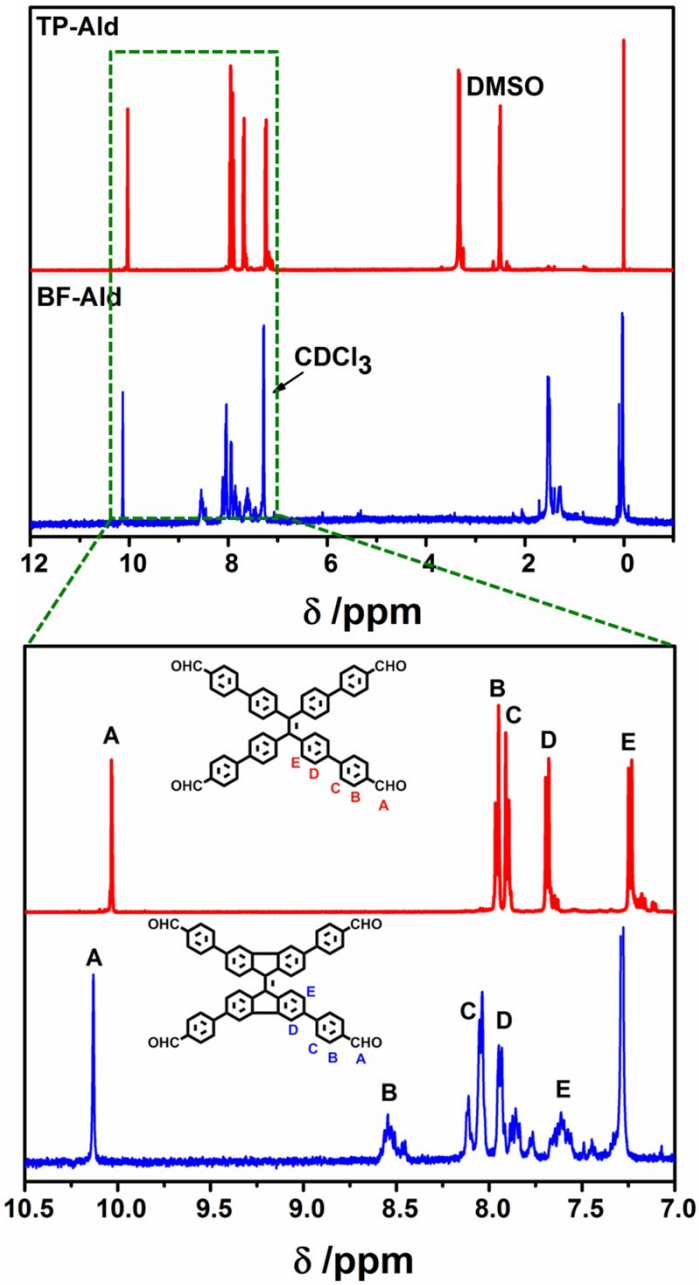

Fig. S24 Comparisonal ^{1}H-NMR spectra of TP-Ald and BF-Ald monomers.

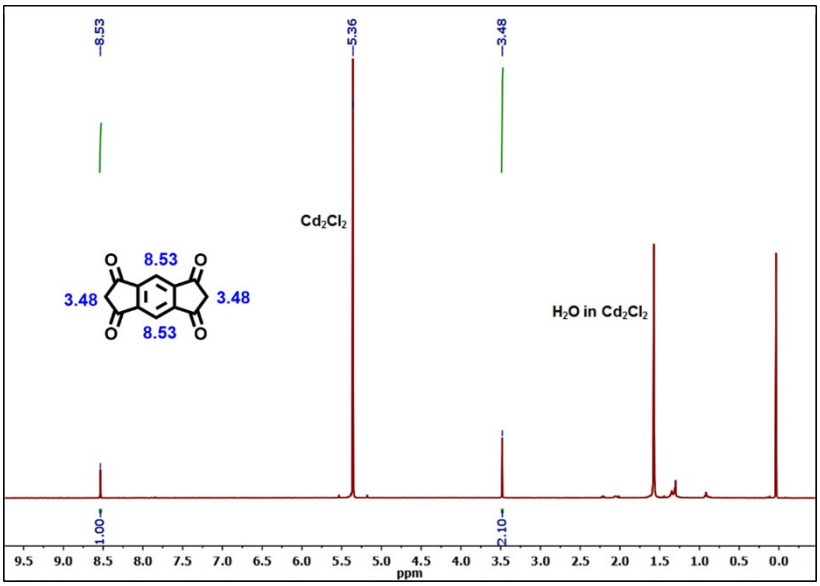

Fig. S25 ^{1}H-NMR spectra of *s*-indacene tetraone.

References

1. R. Francke and R. D. Little, *J. Am. Chem. Soc*, 2013, **136**, 427-435.
2. L. A. Estrada and D. C. Neckers, *J. Org. Chem*, 2009, **74**, 8484-8487.
3. N. Fomina and T. E. Hogen-Esch, *Macromolecules*, 2008, **41**, 3765-3768.
4. F. G. Brunetti, X. Gong, M. Tong, A. Heeger and F. Wudl, *Angew. Chem. Int. Ed*, 2010, **49**, 532-536.
5. P. Krief, J. Y. Becker, A. Ellern, V. Khodorkovsky, O. Neilands and L. Shapiro, *Synthesis*, 2004, **2004**, 2509-2512.
6. L. Zhao, W. Wang, A. Wang, K. Yuan, S. Chen and Y. Yang, *J. Power. Sources*, 2013, **233**, 23-27.
7. H. Wu, K. Wang, Y. Meng, K. Lu and Z. Wei, *J. Mater. Chem. A*, 2013, **1**, 6366-6372.
8. H. Wu, S. A. Shevlin, Q. Meng, W. Guo, Y. Meng, K. Lu, Z. Wei and Z. Guo, *Adv. Mater*, 2014, **26**, 3338-3343.
9. X. Han, C. Chang, L. Yuan, T. Sun and J. Sun, *Adv. Mater*, 2007, **19**, 1616-1621.
10. M. Yao, H. Senoh, S.-i. Yamazaki, Z. Siroma, T. Sakai and K. Yasuda, *J. Power. Sources*, 2010, **195**, 8336-8340.
11. Z. Song, H. Zhan and Y. Zhou, *Angew. Chem. Int. Ed*, 2010, **49**, 8444-8448.
12. Z. Song, H. Zhan and Y. Zhou, *Chem. Commun*, 2009, 448-450.
13. Y. Meng, H. Wu, Y. Zhang and Z. Wei, *J. Mater. Chem. A*, 2014, **2**, 10842-10846.
14. H. Yang, S. Liu, L. Cao, S. Jiang and H. Hou, *J. Mater. Chem. A*, 2018, **6**, 21216-21224.